



# Searches for Long-Lived Particles with Displaced Signatures at the LHC

DANIELA SALVATORE

*Universita' della Calabria and INFN - Cosenza, Dipartimento di Fisica, ponte P. Bucci, 87036 Rende (CS) Italy.*

daniela.salvatore@cern.ch

On behalf of the ATLAS and CMS Collaborations

**Abstract.** This contribution focuses on the most recent results from the ATLAS and CMS Collaborations on the searches for Long-Lived Particles at the Large Hadron Collider. These searches exploit the full dataset collected in 2012 from proton–proton collisions at a center-of-mass energy of 8 TeV. Results can be interpreted in terms of R-parity conserving or violating SUSY models, split SUSY, stealth SUSY and exotic scenarios like Hidden Valley. All the observations are compatible with background expectations and upper limits are set for the cross sections of the different decay modes.

## RESULTS FROM THE ATLAS COLLABORATION

In this section, results from searches performed by the ATLAS experiment [1] are reported.

### Search for Multitrack Displaced Vertices or Displaced Lepton Pairs

Many extensions of the Standard Model (SM) posit the existence of heavy particles with long lifetimes. This search, which is detailed in [2], focuses on events containing two gluinos or two squarks created in the pp collision and at least one long-lived particle (LLP) that decays at distances of the order of mm to tens of cm from its production point, with lifetimes of the order of ps to ns. In the supersymmetric scenarios involving R-parity violation (RPV) and gauge mediation, the LLP is the lightest neutralino ( $\tilde{\chi}_1^0$ ); in the split supersymmetry (split SUSY) the LLP is the gluino. The decay channels under investigation are into two leptons or into five or more charged particles: in the latter case, events are selected using associated lepton candidates, jets or missing transverse momentum ( $E_T^{\text{miss}}$ ). In some of the search channels, the trigger and search strategy are based only on the decay products of individual LLP, irrespective of the rest of the event. In these cases, the provided limits can easily be reinterpreted in different scenarios.

Displaced vertices (DV) are searched starting from the ATLAS standard tracking algorithms, but recovering lost tracks with looser impact parameters. DVs that are situated within regions of dense detector material are vetoed using a three-dimensional map of the detector within the fiducial region (Fig. 1 (left)). The invariant mass  $m_{\text{DV}}$  of all the tracks in the vertex must be greater than 10 GeV. The number of tracks forming the DV is required to be greater than 2 in the di-lepton case and greater than 5 in the multitrack channel.

An example of distribution of events inside or outside the signal region is given at Fig. 1 (right). No events are observed in any of the signal regions in events corresponding to an integrated luminosity of  $20.3 \text{ fb}^{-1}$ , and limits are set on model parameters within the aforementioned scenarios.

### Search for Long-Lived Particles in the Hadronic Calorimeter

In the Hidden Valley (HV) scenario [3] [4] a SM-sector scalar boson  $\Phi$  (that may not necessarily be the SM Higgs boson ( $H$ )) mixes with  $\Phi_{\text{hs}}$ , a hidden sector scalar boson which can decay to v-quarks ( $q_v$ ). The hidden sector consists of a confining gauge group that makes v-hadrons out of its v-quarks, in analogy with QCD. The v-quarks then hadronize to v-particles that can decay back to SM particles. The lightest HV particles  $\pi_v$  are pair-produced and each decays to a pair of SM fermions. The lifetime of the  $\pi_v$  is unconstrained and could be quite long.

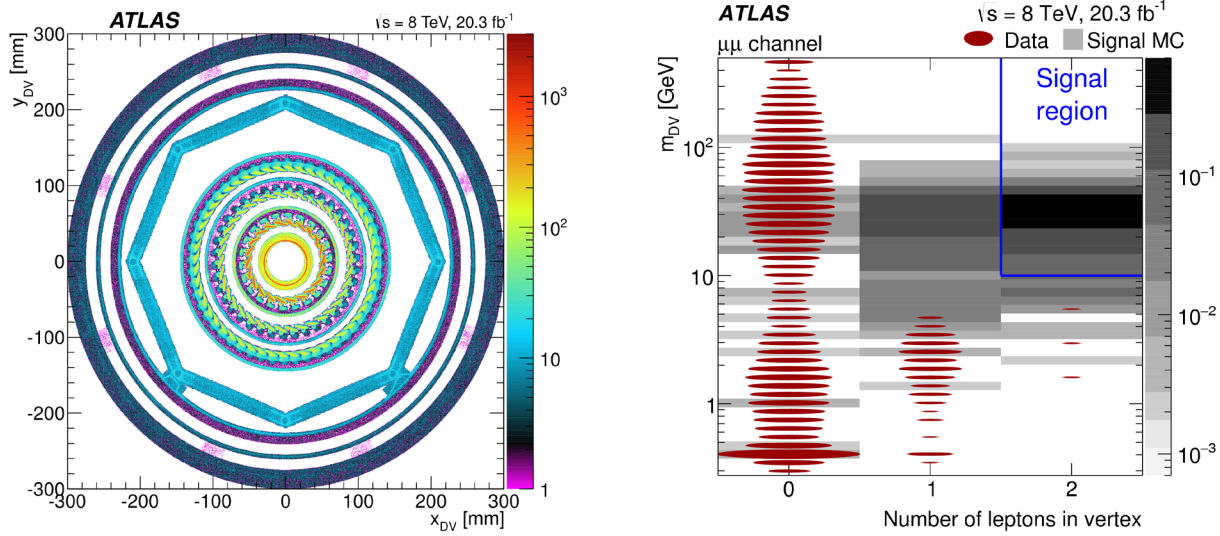


**FIGURE 1.** [2] (left) Transverse-plane density (in arbitrary units) of vertices with fewer than five tracks in material regions that are excluded by the material veto in the region  $|z| < 300$  mm. The innermost circle corresponds to the beam pipe. This is surrounded by the three pixel layers. The octagonal shape and outermost circles are due to support structures separating the pixel and SCT detectors. (right) The distribution of dimuon-vertex candidates in terms of the vertex mass versus the number of lepton candidates in the vertex. The data distributions are shown with red ovals, the area of the oval being proportional to the logarithm of the number of vertex candidates in that bin. The gray squares show the  $\tilde{g}(600\text{ GeV}) \rightarrow q\bar{q} [\tilde{\chi}_1^0(50\text{ GeV}) \rightarrow \mu\mu\nu]$  signal MC sample.

This search [5] focuses on the decay of a scalar boson to a pair of  $\pi_v$  that, in turn, decay at the outer edge of the ATLAS electromagnetic calorimeter (ECal) or inside the hadronic calorimeter (HCal). The  $\pi_v$  are reconstructed as a jet with an unusual energy signature that most traditional searches reject as having poor data quality. This characteristic signature was used to design the dedicated *CalRatio* trigger [6], which looks specifically for LLPs that decay near the outer radius of the ECal or within the HCal. Jets must satisfy  $E_T > 35$  GeV and  $\log_{10}(E_H/E_{EM}) > 1.2$ , where  $(E_H)$  is the energy in the HCal and  $(E_{EM})$  the energy in the ECal. Also they must have no tracks with transverse momentum ( $p_T$ )  $> 1$  GeV in the region  $0.2 \times 0.2$  ( $\Delta\eta \times \Delta\phi$ ) around their axes. Figures 2(a) and (b) show the track multiplicity and the  $\log_{10}(E_H/E_{EM})$  for the signal and background samples.

The signal region is then defined as two simultaneous jets with low electro-magnetic fraction (EMF). No significant excess of events is observed with respect to QCD multi-jet and cosmic ray background events. Limits are reported on the product of the scalar boson production cross section times branching ratio into LLP as a function of the proper lifetime ( $c\tau$ ) of the particles, for boson masses from 100 GeV to 900 GeV, and a LLP mass from 10 GeV to 150 GeV.

## Search for Long-Lived Particles in the Inner Detector and in the Muon Spectrometer

The HV model considers also a massive communicator,  $Z'$ , produced by quark-antiquark annihilation decays into the hidden sector via  $q\bar{q} \rightarrow Z' \rightarrow q_v\bar{q}_v$ . The  $v$ -quarks hadronize into showers of  $\pi_v$  particles where the  $\pi_v^\pm$  lifetime is a free parameter. If a  $\pi_v$  decays in the inner detector (ID) or in the muon spectrometer (MS), it can be reconstructed as a non-standard DV. The stealth SUSY [7] [8] scenario, a class of R-parity-conserving SUSY models that do not have large  $E_T^{\text{miss}}$  signatures, involves adding a hidden-sector (stealth) singlet superfield  $S$  at the electroweak scale, which has a superpartner singlino  $\tilde{S}$ . The SUSY decay chain ends with  $\tilde{S}$  decaying to a singlet plus a low-mass gravitino ( $\tilde{G}$ ), where  $\tilde{G}$  carries off very little energy and the singlet promptly decays to two gluons. The effective decay processes are  $\tilde{g} \rightarrow \tilde{S}g$  (prompt),  $\tilde{S} \rightarrow S\tilde{G}$  (not prompt), and  $S \rightarrow gg$  (prompt). This scenario results in one prompt gluon and two displaced gluon jets per gluino decay resulting in two DVs.

This analysis [9] employs techniques for reconstructing decay vertices of LLP decaying to jets in the ID and MS. Signal events require at least two reconstructed vertices: the dedicated "MuonRoiCluster" trigger [6] is used for the HV scalar boson and stealth SUSY benchmark models decays, where at least one DV must be reconstructed in the MS. A jet +  $E_T^{\text{miss}}$  trigger is used for the HV  $Z'$  benchmark model, for all the combinations of DV in the ID and MS.

No significant excess over the expected background is found and limits as a function of the LLP  $c\tau$  are reported.

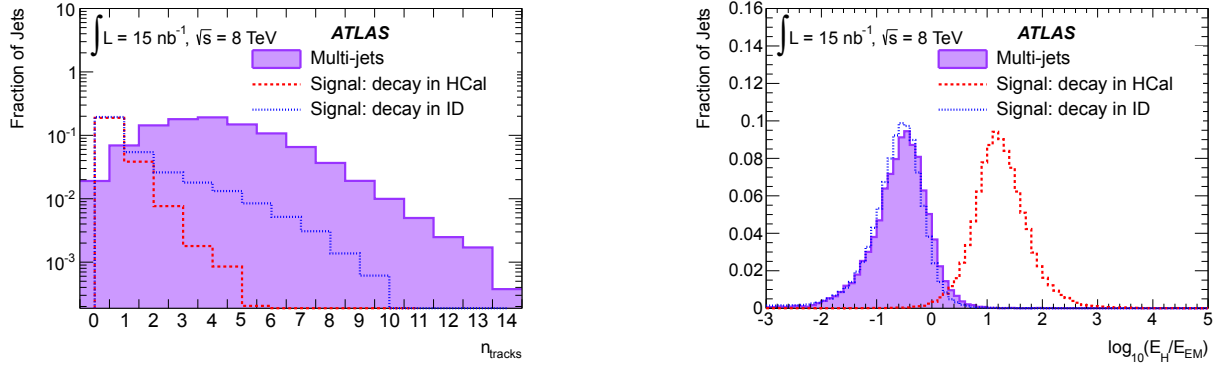


**FIGURE 2.** [5] (left) Number of good tracks ( $n_{\text{tracks}}$ ) with  $p_{\text{T}} > 1$  GeV and  $\Delta R < 0.2$  around the jet axis and (right) jet  $\log_{10}(E_{\text{H}}/E_{\text{EM}})$  with jet  $|\eta| < 2.5$ ,  $p_{\text{T}} > 40$  GeV. The  $\pi_{\nu}$  jets decaying in the HCal or in the inner detector are taken from the  $m_{\text{H}} = 126$  GeV,  $m_{\pi_{\nu}} = 10$  GeV sample. Events are required to satisfy  $E_{\text{T}}^{\text{miss}} < 50$  GeV.

The first results for displaced decays in  $Z'$  and Stealth SUSY models are presented (Fig. 3). For the scalar boson scenario, the upper bounds of the excluded  $c\tau$  are the most stringent to date. Since the current Higgs boson measurement uncertainties do not exclude non-SM decay modes at the 30% or more level, the decay of the SM 125 GeV Higgs boson to a pair of long-lived scalars or pseudo scalars was also explored.

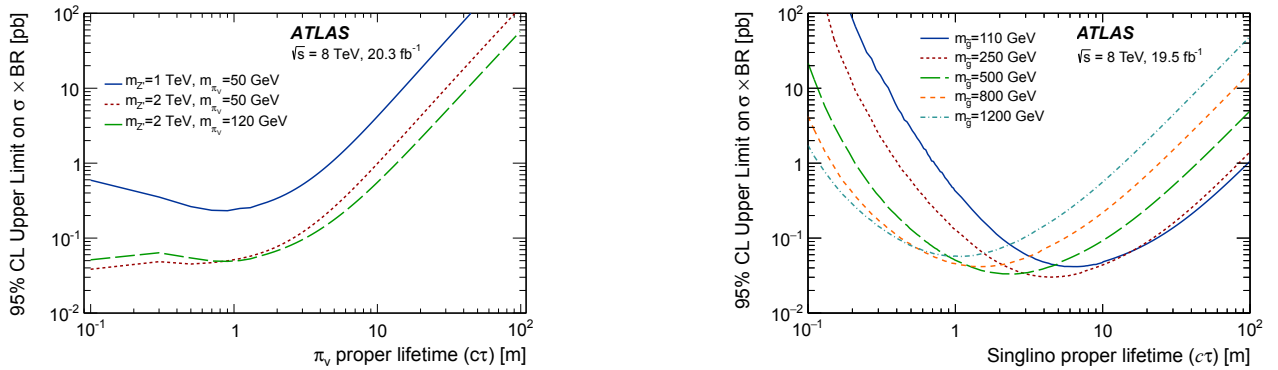


**FIGURE 3.** [9] Observed 95% CL limits on  $\sigma \times \text{BR}$  for the (left)  $Z'$  samples and (right) Stealth SUSY samples.

### Search for Lepton-Jets

In the scenario where the hidden sector and the SM couple via the vector portal, a light hidden photon (dark photon,  $\gamma_d$ ) mixes kinetically with the SM photon. If the hidden photon is the lightest state in the hidden sector, it decays back to SM particles. From  $\gamma_d$  decays, collimated jet-like structures containing pairs of electrons and/or muons and/or charged pions (lepton jets, LJs), and which are produced far from the primary vertex of the event, may arise [10].

A search for LJs in a sample of  $20.3 \text{ fb}^{-1}$  is performed and described in detail in [11]. Three topologies are defined and shown at Fig. 4: LJ-type 0, LJ-type 1 and LJ-type 2. LJ-type 0 select LJs with all  $\gamma_d$  decaying to muons, with  $\gamma_d$  decays beyond the pixel detector up to the first trigger plane of the MS. LJ-type 1 select LJs with one  $\gamma_d$  decaying to a muon pair and one  $\gamma_d$  decaying to an electron/pion pair. The range of decay distances targeted by LJ-type 1 extends from the last ID pixel layer up to the end of the HCal, for  $\gamma_d$  decaying into an electron/pion pair, and from the last ID pixel layer up to the first trigger plane of the MS, for the  $\gamma_d$  decays to muons. LJ-type 2 select all  $\gamma_d$  decaying to electron/pion pairs in the HCal. The requirement of low EMF is needed to reduce the SM multi-jet background.

The two Falkowski-Ruderman-Volansky-Zupan (FRVZ) models [10] predict non-SM Higgs boson decays to LJs and are used as benchmark samples. Since observed events are consistent with background expectations, upper limits

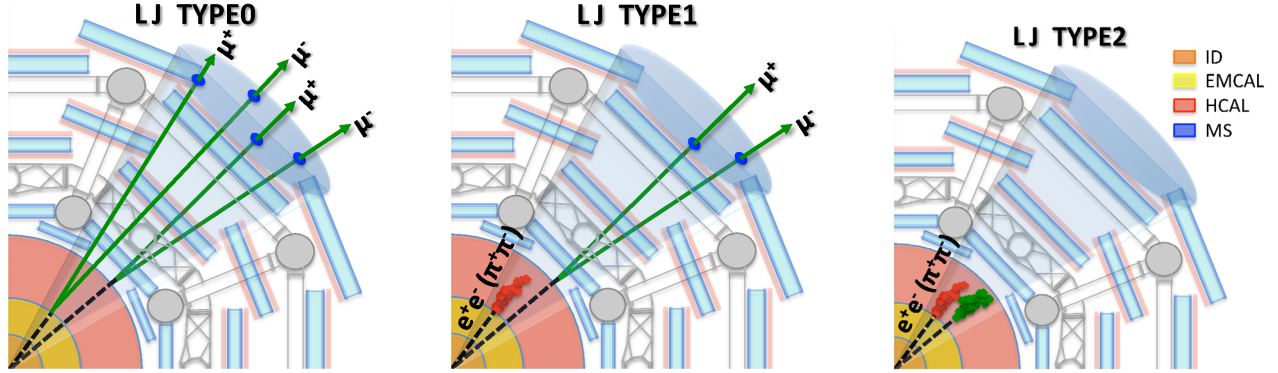


**FIGURE 4.** [11] Schematic picture of the LJ classification according to the  $\gamma_d$  decay final states: left TYPE0 LJ (only muons), centre TYPE1 LJ (muons and jets), right TYPE2 LJ (only jets). LJs containing only one  $\gamma_d$  contribute only to TYPE0 and TYPE2.

are derived as a function of the LLP  $c\tau$ . The range of excluded  $c\tau$  is 52 – 85 mm for the  $H \rightarrow 4 \gamma_d + X$  model: if LJ-type 2 are excluded, this range extends to 15 – 260 mm and is 14 – 140 mm for the  $H \rightarrow 2 \gamma_d + X$  model.

## RESULTS FROM THE CMS COLLABORATION

In this section, results from searches performed by the CMS experiment [12] are reported.

### Search for Long-Lived Particles Decaying into Quark Pairs

A search is performed for massive neutral LLP decaying to quark-antiquark pairs [13]. Quarks fragment and hadronize into jets of particles: therefore, the experimental signature is a distinctive topology of a pair of jets, originating at a secondary vertex that lies within the volume of the CMS tracker and is significantly displaced from the colliding beams. A DV is required to have at least a track from each jet, where constraints are put on the number of tracks with little impact parameters, and a  $m_{DV} > 4$  GeV. A candidate event is shown in Fig. 5.

Results are presented in the context of a HV model [4] where a long-lived, scalar, neutral exotic particle, X, in the mass range of 50 to 350 GeV, decays to  $q\bar{q}$ . The LLP is pair-produced in the decay of a non-SM Higgs boson in the mass range of 200 to 1000 GeV (i.e.  $H \rightarrow 2X, X \rightarrow q\bar{q}$ ), where the H boson is produced through gluon-gluon fusion. In the second model, the LLP is a  $\tilde{\chi}_1^0$  which decays into two quarks and a muon through an RPV coupling. The  $\tilde{\chi}_1^0$  are produced in events containing a pair of squarks, where a squark can decay via the process  $\tilde{q} \rightarrow q \tilde{\chi}_1^0 \rightarrow q q' \bar{q}'' \mu$  [14]. The event selection is optimized for best sensitivity to the H model.

No significant excess is observed above SM expectations in events corresponding to an integrated luminosity of  $18.5 \text{ fb}^{-1}$ . Upper limits at 95% CL are set on the production cross sections for both models. For X with  $c\tau$  of 0.4 to 200 cm, the upper limits are typically 0.5 – 200 fb. For pair production of squarks that promptly decay to  $\tilde{\chi}_1^0$  with  $c\tau$  of 2 – 40 cm, the upper limits on the cross section are typically 0.5 – 3 fb.

### Search for Long-Lived Particles Decaying into Di-leptons

A search is performed for LLP that decay into final states that include a pair of electrons or a pair of muons [15]. In the first benchmark model, the LLP is a spinless boson X, which has a nonzero branching fraction to dileptons. The X is pair-produced in the decay of a non-SM Higgs boson,  $H \rightarrow XX, X \rightarrow \ell^+ \ell^-$  [4], where the Higgs boson is produced through gluon-gluon fusion and  $\ell$  represents either an electron or a muon. In the second model, the LLP is a  $\tilde{\chi}^0$  which can decay via RPV couplings into a neutrino and two charged leptons [14], [16]. The  $\tilde{\chi}^0$  is produced in events containing a pair of squarks, where a squark can decay via the process  $\tilde{q} \rightarrow q \tilde{\chi}^0, \tilde{\chi}^0 \rightarrow \ell^+ \ell^- \nu$ .

The experimental signature is a distinctive topology consisting of a pair of charged leptons originating from a secondary DV. To reject promptly produced particles, the tracks are required to have a transverse impact parameter significance with respect to the primary vertex of  $|d_0|/\sigma_d > 12$ , where  $\sigma_d$  is the uncertainty on  $d_0$ . This value is chosen to give an expected background significantly below one event, which gives the best signal sensitivity for the vast majority of the LLP lifetimes considered. The signed difference in azimuthal angles,  $\Delta\phi$ , between the dilepton

momentum vector,  $\bar{p}_{\ell\ell}$ , and the vector from the primary vertex to the dilepton vertex,  $\bar{v}_{\ell\ell}$ , must satisfy  $\Delta\phi < \pi/2$ , where  $\Delta\phi$  is measured in the range  $0 < \Delta\phi < \pi$ . A comparison between  $|d_0|/\sigma_d$  in signal MC and data is reported in Fig. 6.

No significant excess is observed above SM expectations in events corresponding to an integrated luminosity of 19.6 (20.5)  $\text{fb}^{-1}$  in the electron (muon) channel. Upper limits on the product of the cross section and branching fraction of such a signal are presented as a function of the LLP  $c\tau$ . The limits are presented in an approximately model-independent way, allowing them to be applied to a wide class of models yielding the above topology. In the specific case of a model in which a Higgs boson in the mass range 125 – 1000 GeV decays into a pair of long-lived neutral bosons in the mass range 20–350 GeV, each of which can then decay to dileptons, the upper limits obtained are typically in the range 0.2–10 fb for LLP  $c\tau$  in the range 0.01–100 cm. In the case of the lowest Higgs mass considered (125 GeV), the limits are in the range 2–50 fb. These limits are sensitive to Higgs boson branching fractions as low as  $10^{-4}$ .

### Search for Long-Lived Particles in the Muon Chamber only

This study, described in [17], is closely related to the analysis described right above, since similar analysis techniques are employed to search for the same signal topology. While the previous analysis relied on electrons or muons whose trajectories were reconstructed in the silicon tracker, this study is based on information from muon tracks reconstructed in the CMS muon chambers only, which are able to reconstruct muons produced an order of magnitude farther away from the beam-line than what the silicon tracker can. This search improves sensitivity to particles that are especially long-lived and is fully complementary to the tracker-based one, since it explicitly excludes any muon whose trajectory is reconstructed in the silicon tracker and combined results from the two searches are presented.

No events corresponding to an integrated luminosity of 20.5  $\text{fb}^{-1}$  pass the selection criteria for each of the two specific aforementioned benchmark models. Upper limits on the product of the cross section and branching fraction of such a signal are presented as a function of the LLP  $c\tau$ . For the first model, where a Higgs boson with mass in the range 125 – 1000 GeV decays to pairs of neutral LLP with masses in the range 20 – 350 GeV, that can decay to dimuon pairs, the limits are typically in the range 1 – 50 fb, and can weaken to a few pb for the lowest masses and longest lifetimes. Upper limits are given for lifetimes in the range  $1 < c\tau < 10000$  cm.

### Search for Events with an Electron and a Muon with Large Impact Parameters

A search for new LLP decaying to leptons is presented [18], using an integrated luminosity of 19.7  $\text{fb}^{-1}$ . This search does not make any assumptions about the event topology beyond the requirement that the event contain an isolated electron and isolated muon with large impact parameters (between 0.02 and 2 cm) and opposite charges. It does not require, or exclude, hadronic activity or  $E_T^{\text{miss}}$ , neither that the reconstructed displaced tracks form a vertex. It does not require that the displaced tracks are collimated. In this way, the analysis has sensitivity to a wide variety of still viable beyond SM scenarios.

No excess is observed above background for displacements up to 2 cm. The results are interpreted in the context of a “displaced supersymmetry” model [19] with a pair-produced top squark decaying into an  $e-\mu$  final state via RPV

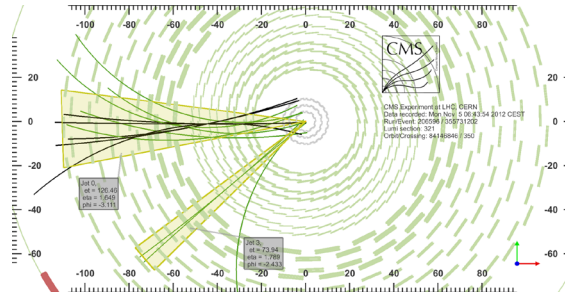


**FIGURE 5.** [13] Event display of a candidate in data, where only the selected dijet pair (yellow cones) and the tracks associated to both jets (curved lines) are shown, other objects being removed. The black tracks fit the secondary vertex which contains 5 tracks (5 from one jet and 2 from the other, while 2 tracks are associated to both jets) and is transversely displaced by 44 cm from the event primary vertex. The invariant mass of the dijet system is 75 GeV.

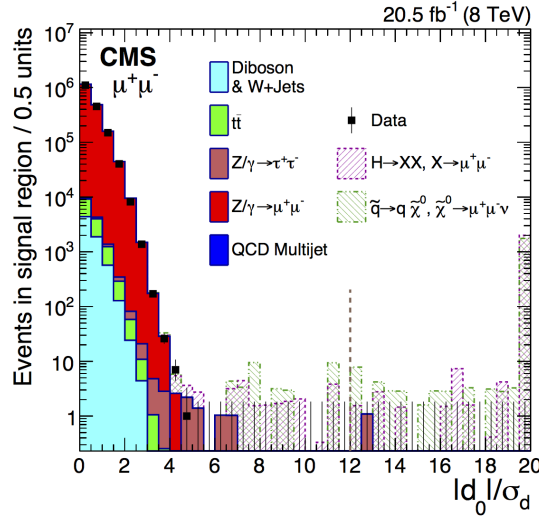


**FIGURE 6.** [15] The  $|d_0|/\sigma_d$  distribution for the muon channels for events in the signal region  $|\Delta\phi| < \pi/2$ . Of the two leptons forming a candidate, the distribution of the one with the smallest  $|d_0|/\sigma_d$  is plotted. The solid points indicate the data, the shaded histograms are the simulated background, and the hashed histograms show the simulated signal. The histogram corresponding to the  $H \rightarrow XX$  model is shown for  $m_H = 1000$  GeV and  $m_X = 350$  GeV. The histogram corresponding to the  $\tilde{\chi}^0 \rightarrow \ell^+ \ell^- \nu$  model is shown for  $m_{\tilde{q}} = 350$  GeV and  $m_{\tilde{\chi}^0} = 140$  GeV. The background histograms are stacked, and each simulated signal sample is independently stacked on top of the total simulated background. The  $d_0$  corrections for residual tracker misalignment, discussed in the text, have been applied. The vertical dashed line shows the selection requirement  $|d_0|/\sigma_d > 12$ . Any entries beyond the right-hand side of a histogram are shown in the last visible bin of the histogram.

interactions, having a lifetime  $0.02 < c\tau < 100$  cm. Limits are placed at 95% CL on this model as a function of top squark mass and lifetime. For a lifetime hypothesis of  $c\tau = 2$  cm, top squark masses up to 790 GeV are excluded.

## REFERENCES

- [1] ATLAS Collaboration, JINST 3, S08003 (2008).
- [2] ATLAS Collaboration, Phys. Rev. D 92, 072004 (2015).
- [3] M. J. Strassler and K. M. Zurek, Phys. Lett. B 651 (2007) 374–379.
- [4] M. J. Strassler and K. M. Zurek, Phys. Lett. B 661 (2008) 263–267.
- [5] ATLAS Collaboration, Phys. Lett. B 743 (2015) 15–34.
- [6] ATLAS Collaboration, JINST 8 (2013) P07015.
- [7] J. Fan, M. Reece, and J. T. Ruderman, JHEP 1111 (2011) 012.
- [8] J. Fan, M. Reece, and J. T. Ruderman, JHEP 1207 (2012) 196.
- [9] ATLAS Collaboration, Phys. Rev. D 92 (2015) 012010.
- [10] A. Falkowski, J.T. Ruderman, T. Volansky and J. Zupan, JHEP 05 (2010) 077.
- [11] ATLAS Collaboration, JHEP 11(2014) 088.
- [12] CMS Collaboration, JINST 3 S08004 (2008).
- [13] CMS Collaboration, Phys. Rev. D 91 (2015) 012007.
- [14] R. Barbieri et al., Phys. Rep. 420, 1 (2005).
- [15] CMS Collaboration, Phys. Rev. D 91 (2015) 052012.
- [16] B. C. Allanach et al., Phys. Rev. D 75, 035002 (2007).
- [17] CMS Collaboration, CMS PAS EXO-14-012 (2014).
- [18] CMS Collaboration, PRL 114, 061801 (2015).
- [19] P. W. Graham et al., JHEP 07 (2012) 149.
- [20] M. Cacciari, G. P. Salam and G. Soyez, JHEP 0804 (2008) 0633.
- [21] A. Read, J. Phys. G 28 (2002) 2693.
- [22] ATLAS Collaboration, ATLAS-CONF-2010-069.